Interaction of surface radiation with free convection in a square cavity

C. Balaji and S. P. Venkateshan
Indian Institute of Technology, Madras, India

A numerical investigation of free convection in a rectangular enclosure has been carried out based on Gosman's finite volume method with a 21 × 21 nonuniform grid. A radiation model has been included in the analysis to study the effect of surface radiation on the heat transfer characteristics of the enclosure. The model is general since it takes into account different emissivities for the side walls and for the top and bottom walls. The nonuniform grids for convection have been retained for radiation, notwithstanding the fact that the evaluation of view factors becomes highly tedious. The view factors are evaluated by Hottel's crossed-string method. Nonuniform grids for both convection and radiation routines ensure grid compatibility and yield convergent solutions. The model has thrown light onto the importance of surface radiation even at low emissivities and temperature levels and provides an explanation of the discrepancies between the experimental and theoretical correlations. A parametric study of surface radiation effects is also presented.

Keywords: radiation convection interaction; radiation Nusselt number; convective drop; radiosity

1. Introduction

The problem of free convection in enclosed spaces has been extensively studied because of its importance in many practical applications such as the design of solar collectors, energy efficient buildings, the cooling of electronic equipment, and a host of others. Although in most cases the flow is three-dimensional (3-D), two-dimensional (2-D) results are often satisfactory, especially considering the large reduction in computational effort. In most cases, there is an interaction of surface radiation and free convection, and in many of the analyses this interaction is omitted by "alleging" that once the emissivities chosen are low, then radiation can be neglected. In some cases, the radiation contribution has been taken care of by adding a "correction" using simple formulae like that between infinite parallel plates facing each other (Hoogendoorn 1985). The errors that arise because of the above approximations and highlighting of the "dual" nature of surface radiation, viz. interaction with free convection and vice versa, are the main thrusts of the present paper. A careful review of the literature suggests that the work of Asako and Nakamura (1982) is one of the very few earnest attempts to probe into the effect of surface radiation on free convection in an enclosure. However, they used a 10 × 10 uniform-size grid for both convection and radiation, and the heat transfer from the top wall was assumed to be equal to the heat transfer from the bottom wall. In the present work, a finer mesh has been used near the walls, with progressively coarser meshes towards the core (grid used: 21 × 21). Also, more realistic boundary conditions for temperature have been used for the top and bottom walls. The results we have obtained tend to explode the common myth that corrections could be made for the radiation heat transfer by adding the radiation with the simpler formulae. We also show that even at low emissivities, radiation plays a significant and "dual" role in that it brings down the convective component, even though the net heat transferred across the enclosure may be increased or decreased depending on the particular radiative parameters.

Address reprint requests to Professor Venkateshan at the Heat Transfer and Thermal Power Laboratory, Department of Mechanical Engineering, Indian Institute of Technology, Madras 600 036, India.

Received 22 July 1992; accepted 9 November 1992

2. Formulation of the problem

The central theme of the present work is the study of the effect of surface radiation on free convection in a square cavity, however, to provide greater confidence in the present results, the pure convection code is validated first. The results are in excellent agreement with the previous workers (see Figure 3). Hence, for the sake of completeness, we present the governing equations along with the necessary boundary conditions for both the pure convection problem and the combined convection and radiation problem. The governing equations for steady, laminar, constant property flow for a square cavity with end walls at different temperatures and top and bottom walls insulated assuming Boussinesq approximation to be valid (see Figure 1) are reported in a number of references (e.g., Bejan 1984). The governing equations can be simplified using the stream function-vorticity formulation. The governing equations in normalized form are

$$u\frac{\partial W}{\partial X} + V\frac{\partial W}{\partial Y} = \mathrm{Pr}[\nabla^2 W] - \mathrm{Ra}\frac{\partial \phi}{\partial Y} \tag{1}$$

$$\nabla^2 \psi = -\mathrm{Pr}\, W \tag{2}$$

$$\nabla^2 \phi = U\frac{\partial \phi}{\partial x} + V\frac{\partial \phi}{\partial Y} \tag{3}$$

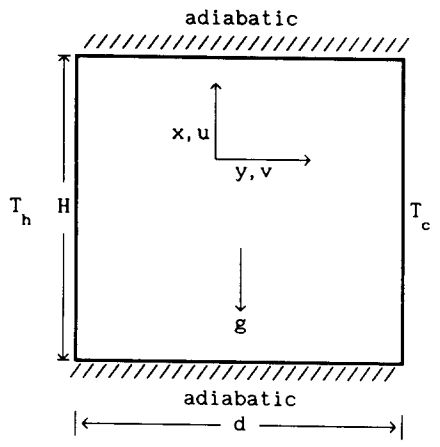

Figure 1 Sketch of the enclosure

The boundary conditions are

$X = 0, 2$, for all Y $\quad \psi = 0$ (4a)

$Y = 0, 2$, for all X $\quad \psi = 0$ (4b)

$Y = 0$, for all X $\quad \phi = 1$ (4c)

$Y = 2$, for all X $\quad \phi = 0$ (4d)

$X = 0, 2$, for all Y $\quad \dfrac{\partial \phi}{\partial X} = 0$, for the pure convection problem (4e)

$X = 0, 2$, for all Y $\quad \dfrac{\partial \phi}{\partial X} = N_{RC} q_R / \sigma T_h^4$, for the combined convection and radiation problem (4f)

3. Radiosity formulation

For the radiosity formulation, the nonuniform grids used for convection have been retained to ensure grid compatibility. The non-dimensional radiosity equation for the ith of the 80 elements (for a 21 × 21 grid, there are 20 elements on each wall) on the wall is given by

$$j_i = \varepsilon_i + (1 - \varepsilon_i) \sum_{j=1}^{80} F_{ij} j_j, \; i = 1 \text{ to } 80 \tag{5}$$

where F_{ij} is the view factor from the ith to the jth element.

Since there are three equations for three variables—vorticity, stream function, and temperature—and the respective equations are elliptic, we need four additional boundary conditions on vorticity to close the problem. To generate these boundary conditions, we start with the assumption that the stream function equation is satisfied at the walls. Then an assumption is made that gradients parallel to the wall are negligible in comparison with those perpendicular to the wall. In this manner four additional boundary conditions are generated. In the present study, in view of the nonuniform grid employed, Lagrangian polynomials have been used to obtain three point formulae for wall vorticity conditions.

The above boundary-condition generation for vorticity gives a clear indication of the tediousness associated with the vorticity method when encountering complicated geometries like the presence of multiple partition plates. Notwithstanding the fact that the vorticity method offers very unique features, such as elimination of the troublesome pressure terms and the physical significance of vorticity in a recirculating flow like this, the complications in generating boundary conditions each time a wall or a free boundary (e.g., an opening) is encountered does place this method at a definite disadvantage *vis-à-vis* the primitive variable method, particularly for complicated geometries.

Notation

a	Constant in the Nusselt number correlation
b	Exponent of Grashof number in the Nusselt number correlation
d	Spacing, m
g	Acceleration due to gravity, m/s^2
Gr	Grashof number based on d, $g\,\beta(T_h - T_c)d^3/\nu^2$
H	Height of the enclosure, m
j	Nondimensional radiosity, $J/\sigma\, T_h^4$
J	Radiosity, W/m^2
k	Thermal conductivity of fluid, W/m K
N_{RC}	Radiation conduction interaction parameter, $\sigma T_h^4 d/[k(T_h - T_c)]$
Nu_f	Local Nusselt number, $-(\partial\phi/\partial Y)_{y=0}$
$\overline{\mathrm{Nu}}_f$	Average or mean Nusselt number, $\int_0^2 \mathrm{Nu}_f\, dX/2$
Nu_R	Radiation Nusselt number, $(q_R d)/[k(T_h - T_c)]$
$\overline{\mathrm{Nu}}_R$	Average or mean radiation Nusselt number, $\int_0^2 \mathrm{Nu}_R\, dX/2$
Nu_O	Overall Nusselt number, Nu_f (with radiation) + Nu_R
Pr	Prandtl number, ν/α
q_R	Radiative heat flux, $[\varepsilon/(1-\varepsilon)][\sigma T^4 - J]$, W/m^2
Ra	Rayleigh number based on d, Gr Pr
T	Temperature at any location (X, Y), K
T_r	Temperature ratio, T_c/T_h
u	Vertical velocity, m/s
U	Nondimensional vertical velocity, ud/α
v	Horizontal or cross velocity, m/s
V	Nondimensional horizontal velocity, vd/α
W	Nondimensional vorticity, $\omega d^2/\nu$
x	Vertical distance, m
X	Nondimensional vertical distance, $2x/d$
y	Horizontal distance, m
Y	Nondimensional horizontal distance, $2y/d$

Greek symbols

α	Thermal diffusivity, m^2/s
β	Thermal expansion coefficient, 1/K
ε	Emissivity
ν	Kinematic viscosity, m^2/s
ϕ	Dimensionless temperature, $(T - T_c)/(T_h - T_c)$
ψ	Dimensionless stream function, ψ'/α
ψ'	Stream function, m^2/s
ω	Vorticity, 1/s

Subscripts

h	Hot wall
c	Cold wall
t	Top wall
b	Bottom wall

4. Method of solution

4.1. Pure convection problem

Based on the Gosman et al (1969) finite-volume method, a code has been developed for solving the nondimensional equations. Suitable nondimensionalization shows that the number of input parameters to be specified is reduced to two, namely, the Rayleigh number and the Prandtl number. From our computation we have observed that Prandtl number is not a significant parameter, at least in the range of Prandtl numbers (0.2–20) covered in the present study (see Shembarkar et al. 1977). An important feature of the solution procedure is the use of upwinding while handling convection terms. The use of upwinding ensures that convection coefficients in the algorithm are always positive—at the worst zero, but never negative—thus ensuring convergent solutions.

A 21 × 21 nonuniform grid has been generated using a cosine function. The use of a cosine function gives very fine grids near the walls and progressively coarser grids towards the core. The grid pattern of the left bottom quadrant of the enclosure is shown in Figure 2. As regards the implementation of the derivative boundary conditions, three-point formulae using a Lagrangian polynomial of degree 2 have been used. This procedure, coupled with a very fine grid near the walls, makes the derivative boundary conditions on the wall less prone to error.

For all the equations, underrelaxation has been used. Initial trial runs have shown that the use of a relaxation parameter greater than one leads to divergence. A relaxation parameter of 0.5 has been found to give convergent results for a wide range of aspect ratios and Rayleigh numbers in the present study, and hence has been used throughout. It is noted in passing that a relaxation parameter of 0.5 corresponds to the Crank–Nicholson method in finite differences, which is a balanced implicit–explicit method.

A convergence criterion of 0.01 percent has been used for Ra = 1,000. This is more stringent than the value of 0.1 percent recommended by De Vahl Davis and Jones (1983). As with any numerical method, the accuracy of the solution reduces with Ra. In the present study, the maximum error at Ra = 10^6 has been found to be 0.8 percent for the temperature, with the number of iterations limited to 600.

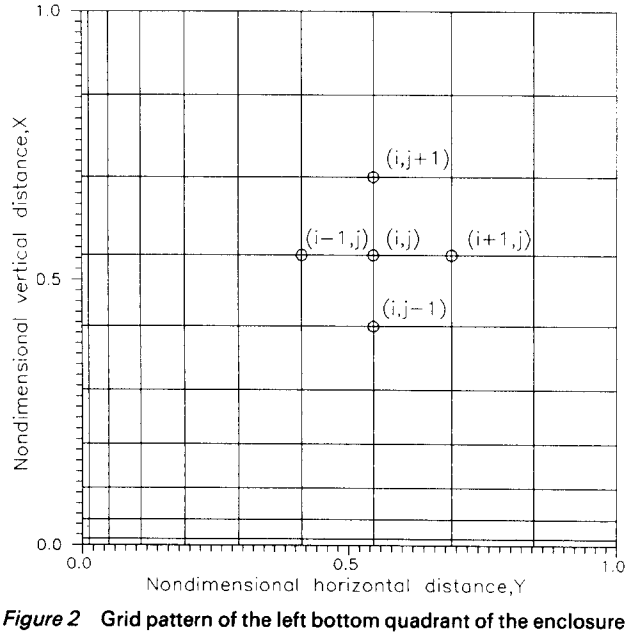

Figure 2 Grid pattern of the left bottom quadrant of the enclosure

After the velocity and temperature distributions are obtained, the local Nusselt numbers are found by using the Lagrangian polynomial of second degree, and the mean Nusselt numbers have been evaluated using numerical integration with an extended trapezoidal rule for nonuniform step sizes.

4.2. Combined convection and radiation problem

The solution procedure for the combined problem is the same as that for a pure convection problem, but with the necessary modifications on the boundary conditions for the top and bottom walls. These boundary conditions are nonlinear in temperature, aside from the fact that the radiosities themselves are functions of temperature. The radiosities are obtained by solving the radiosity equations for an enclosure as reported in Hottel and Sarofim (1967). The view factors have been evaluated using Hottel's crossed-string method. The nonlinear boundary conditions on the adiabatic top and bottom walls are solved for using an explicit finite-difference technique. The radiosity equations have been solved by the Gaussian elimination technique, which is a direct solver. Once the boundary conditions are established, the next iteration for the convection equations is performed, then the whole process is repeated until the required convergence is obtained.

Calculations have been performed for the typical ranges of the various parameters that enter the problem, as shown in Table 1. A specific case of Ra = 50,000 has been chosen for the detailed study of the effects of other parameters on the heat transfer characteristics of the enclosure.

5. Results and discussion

5.1. Comparison for the pure convection case

For the case of a square cavity, a plethora of results are quoted in the literature. A comparison of the existing correlations along with the data spread of the present work is given in Figure 3. The average Nusselt number is usually correlated by a formula of the form $Nu_f = a\ Gr^b$ for air. It is appropriate to mention here that the Grashof number has been used in order to facilitate comparison with other workers. Also, we would like to reiterate that in the Prandtl number range covered, the Prandtl number does not play a significant role, i.e., different fluids will give the same Nusselt number for a given Rayleigh number (for the present study, $0.2 < Pr < 20$). Table 2 shows the values of a and b pertaining to the studies indicated in Figure 3. The correlations of Newell and Schmidt (1970) and Han (1967) report excessively large values of the Grashof number exponent b—0.397 and 0.359, respectively—in their Nusselt number correlations, as is clear from the steep slopes of these correlations in Figure 3. Landis and Rubel (1970) noted this and attributed it to the use of uniform grids in the calculations. Specifically, at large Rayleigh numbers, uniform grids are prone to excessive errors as the boundary layer

Table 1 Typical ranges of parameters for the combined convection and radiation problem

Parameter	Range
Prandtl number	$0.2 < Pr < 20$
Rayleigh number	$500 < Ra < 10^6$
Emissivity (side walls)	$0.1 < \varepsilon_h = \varepsilon_c < 0.95$
Radiation conduction interaction parameter	$0.5 < N_{RC} < 5$
Temperature ratio	$0.7 < T_r < 0.98$

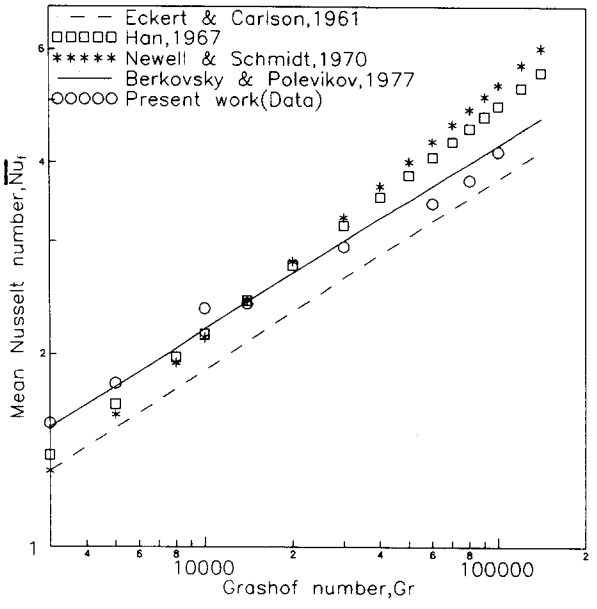

Figure 3 Comparison of the existing Nusselt number correlations for air along with the present data

becomes more and more slender and convergent solutions with high accuracies are not obtainable. In fact Berkovsky and Polevikov (1977) used a fourth-order-accurate scheme precisely for this reason and obtained a Grashof number exponent b of 0.29. Thus it may be concluded that the present results, which are in excellent agreement with those of Berkovsky and Polevikov (1977)—who are reported by Gebhart et al. (1988) to have the most accurate correlation—are a clear indication of the soundness of the convection code, and the incorporation of surface radiation in the code is expectedly fairly accurate.

On the experimental side, the widely quoted correlation of Eckert and Carlson (1961) runs well below all the other correlations, although the Grashof number exponent in their work (0.30) is in good agreement with that of the present work (0.305) and that of Berkovsky and Polevikov (0.29). An attempt to explain the discrepancies between the experimental and numerical predictions will be made in section 5.8 below. We would like to mention here that in Eckert and Carlson's work, the experiments were performed over a few representative values of height-to-width ratio. But Eckert and Carlson have proposed two correlations for the Nusselt number, one containing the height-to-width ratio, and the other without it. We have used their second correlation for purposes of comparison. However, extrapolation of their results to aspect ratios (height to width) for which experiments have not yet been performed may be questionable.

Table 2 Values of a and b from studies indicated in Figure 3 ($\overline{Nu}_f = a\,Gr^b$)

Source	a	b
Eckert & Carlson	0.119	0.30
Han	0.0782	0.359
Newell & Schmidt	0.0547	0.397
Berkovsky & Polevikov	0.15	0.29
Present work	0.13	0.305

5.2. The effect of surface radiation on Nusselt number

In the preceding section we have presented results for a square cavity and have given a brief comparison of the present results with the existing numerical and experimental correlations. A striking feature of this comparative analysis has been that experimental correlations in general tend to disagree with theoretical correlations, as pointed out here and in Bejan (1984). From a careful study of previous experimental works, one can see that in many of them, either the radiation contribution has been disregarded altogether or some sort of a correction has been introduced by a simple formula, such as $\sigma(T_h^4 - T_c^4)/(1/\varepsilon_h + 1/\varepsilon_c - 1)$. Because the present geometry is an enclosure, there are multiple reflections all along its boundaries. Hence the parallel-plate formula above does not predict the radiation Nusselt number accurately. The magnitude of the errors depend on the particular combination of the radiative parameters, viz. the ε's, T_r, and N_{RC}. This aspect will be discussed in more detail in sections 5.5 to 5.7.

With this background, we present below results that elucidate the effect of surface radiation on Nusselt number. We have chosen a Rayleigh number of 50,000 as the standard case, since it is known that at such a Rayleigh number the flow is in the boundary-layer regime. Figure 4 highlights the variation of the local-convection Nusselt number without and with radiation for $\varepsilon_h = \varepsilon_c = 0.10$ and $\varepsilon_t = \varepsilon_b = 0.90$. We have purposely chosen this combination because in experimental investigations of natural convection in cavities, the side walls are usually made of polished copper or aluminum and the top and bottom walls are made of asbestos, balsa wood, or some other suitable insulating material (Eckert and Carlson 1961). The Nusselt number distribution (Figure 4) clearly shows that surface radiation leads to a drop in the convective component, a phenomenon that will be referred to hereafter as the *convective drop*. However, this reduction tends to be compensated for by radiative transfer between the hot and cold walls. Hence, the net effect of radiation can be to increase or decrease the overall heat transfer across the enclosure, depending upon the interplay between the convection and the radiation. We will say more about this point a little later (section 5.5). Hence, surface radiation has a "dual" role to play, and the superposition of

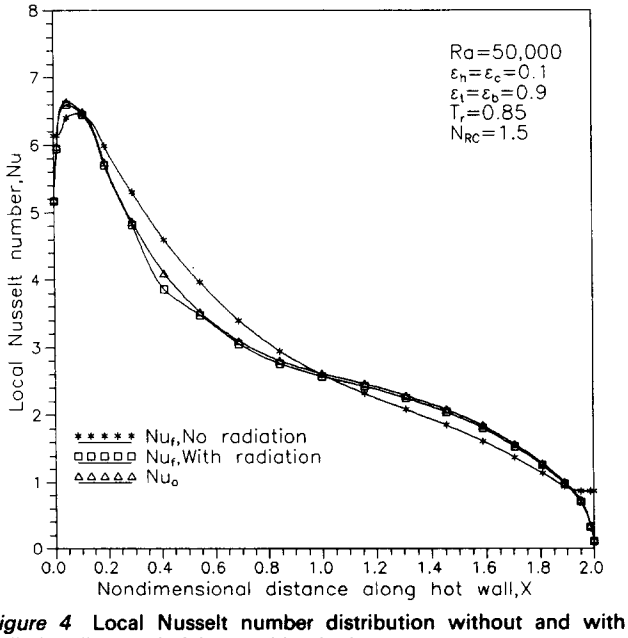

Figure 4 Local Nusselt number distribution without and with radiation (low emissivity combination)

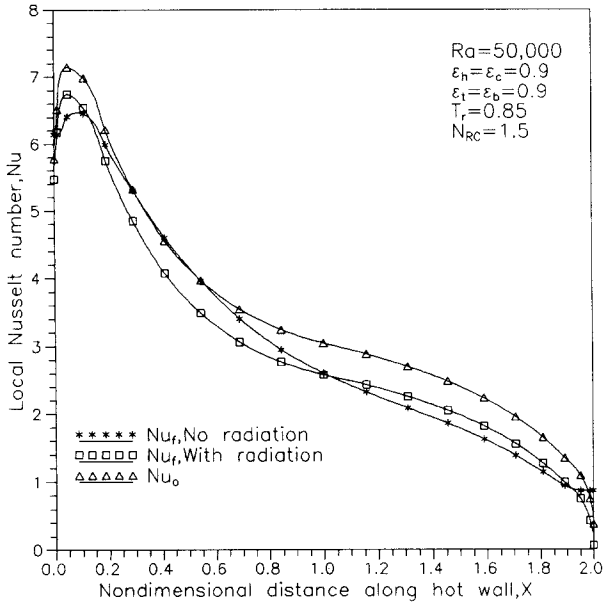

Figure 5 Local Nusselt number distribution without and with radiation (high emissivity combination)

convection and radiation, as done in previous studies, is in error. The error becomes more severe as radiation becomes more dominant, as in the case of high wall emissivities and higher N_{RC}'s. Similar results are shown in Figure 5, but for a higher emissivity combination ($\varepsilon_h = \varepsilon_c = \varepsilon_t = \varepsilon_b = 0.9$) at the same Rayleigh number of 50,000. It can be seen that the overall Nusselt number (the sum of the convective component with radiation and the radiative component) for this case is *more* than that for a pure convection case. The mean radiation Nusselt number for this combination of fixed parameters, but with ε_h as a variable, correlated as $Nu_R = 0.48\varepsilon_h^{1.09}$ with a correlation coefficient of 0.998 and a standard deviation of 0.028. Figure 6 clearly shows that the modified radiation Nusselt number ($Nu_R/\varepsilon_h^{1.09}$) varies quite strongly with position along the hot wall. The simpler formulae would assume a uniform value of radiosity and give a mean radiation Nusselt number that is different from the presently calculated one. We reiterate our earlier statement that for higher wall emissivities and higher N_{RC}'s, the error is more severe. We will elaborate on this point in section 5.6. One of the major conclusions to be drawn from the figures is that for the case of low ε, the convection drop could be 6 to 7 percent even at moderate values of N_{RC}'s like 1.5, but for the high emissivity case, although the convection drop could be less than this, the mean radiation Nusselt number can be 15 to 18 percent of the mean convection Nusselt number. Hence, even at normal temperature levels and relatively low emissivities and N_{RC}'s, the effect of surface radiation is to swing the overall Nusselt number up to 10 percent either way. This clearly attempts to remove the haziness that shrouds the discrepancies between numerical and experimental correlations. Minor effects like three-dimensionality and nonuniform temperature of the side walls can also play a role in causing the aforementioned discrepancy (Asako and Nakamura 1982). However, we use a very specific example in section 5.8 to show that surface radiation is the major reason for the discrepancy.

5.3. Temperature and radiosity distribution

To gain further physical insight into the problem, we now look at the temperature and radiosity profiles. Figures 7 and 8 highlight the variation of top and bottom surface-temperature profiles, respectively, for the low and high emissivity cases. It is clear, firstly, that the surface radiation has not really affected the symmetry of the profile very much. Secondly, the top wall is affected more by radiation than the bottom wall. The top wall registers a general increase in temperature values as a result of radiation, as opposed to the bottom wall, which registers a slight decrease in temperature values near the cold wall region, i.e., towards the right end of the enclosure. Figure 9 shows the midplane temperatures for the two cases of low and high emissivities as opposed to the case for pure convection. These results clearly show that radiation equilibriates the temperature in the enclosure and hence the drop in convective Nusselt number takes place as expected. Figures 10 and 11 highlight the variation of nondimensional radiosities along the side walls

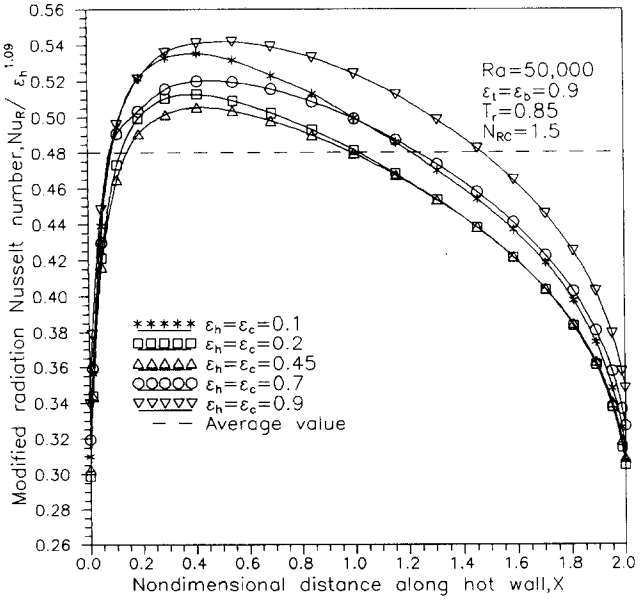

Figure 6 Modified radiation Nusselt number distribution along hot wall

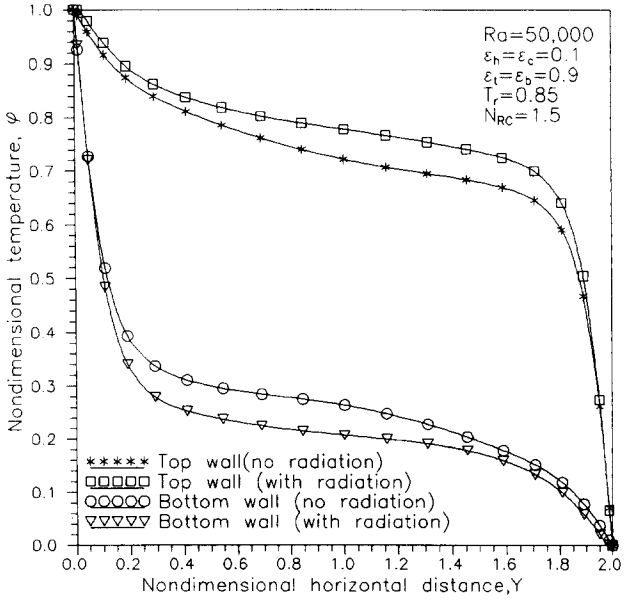

Figure 7 Nondimensional temperature distribution along the adiabatic walls of the enclosure (low emissivity combination)

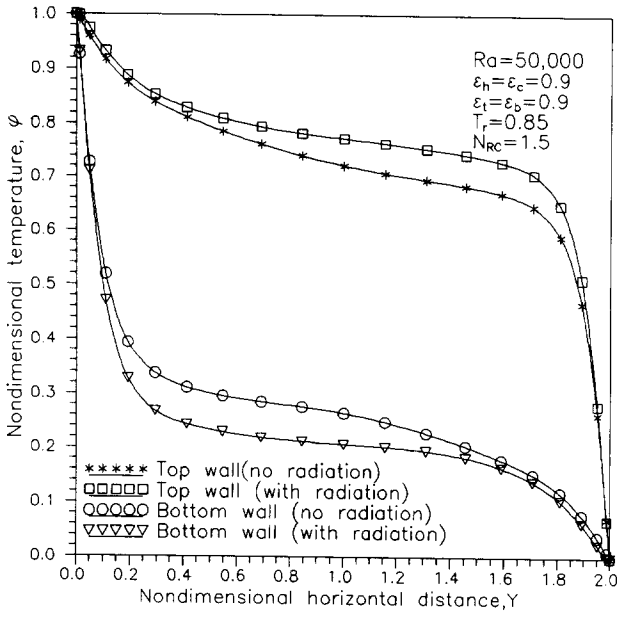

Figure 8 Nondimensional temperature distribution along the adiabatic walls of the enclosure (high emissivity combination)

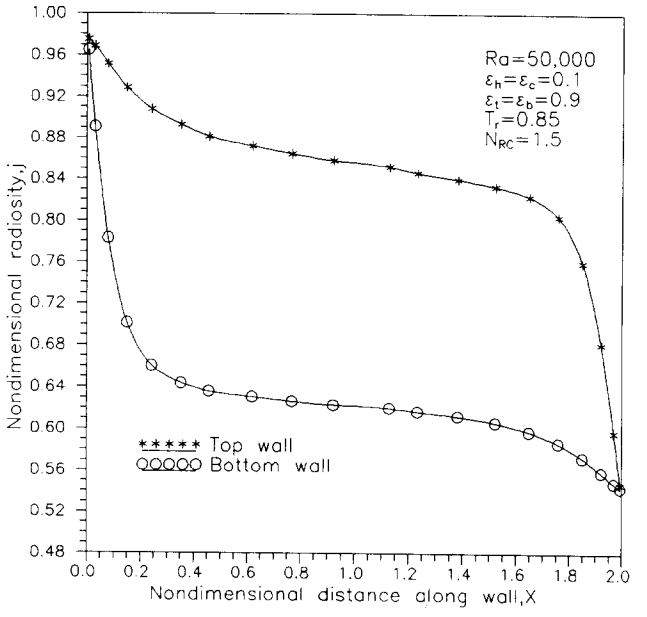

Figure 10 Nondimensional radiosity distribution along the adiabatic walls (low emissivity combination)

and the top and bottom walls, respectively. The similarity between the temperature and radiosity profiles is indeed striking. More importantly, the radiosity distribution of the side walls highlights certain subtle points. Mere isothermality of a wall does not ensure that the radiosities are uniform along the wall. Also, unlike gas radiation, surface radiation does not affect the symmetry of the temperature about a vertical midplane (Lauriat 1991; Yang and Lloyd 1985).

5.4. *The effect of Rayleigh number on convective drop*

Table 3 sums up the effect of radiation for two representative Rayleigh numbers of 50,000 and 75,000, with the other parameters fixed at values corresponding to those in previous figures.

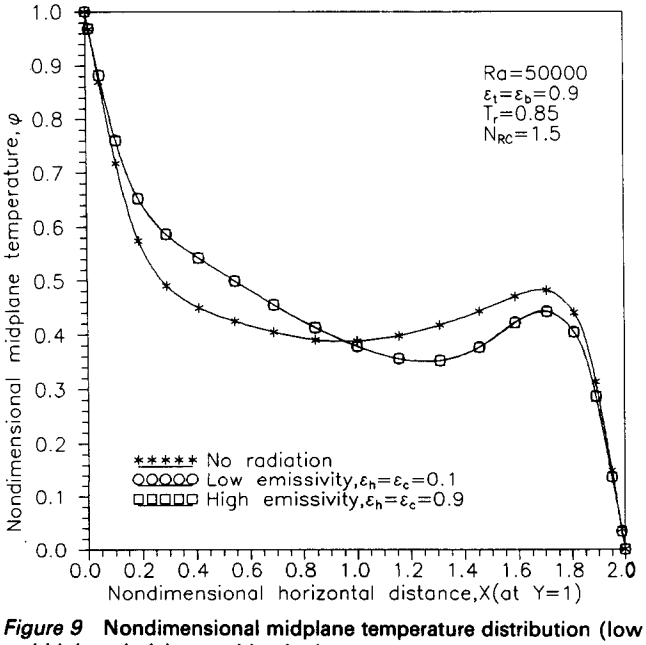

Figure 9 Nondimensional midplane temperature distribution (low and high emissivity combination)

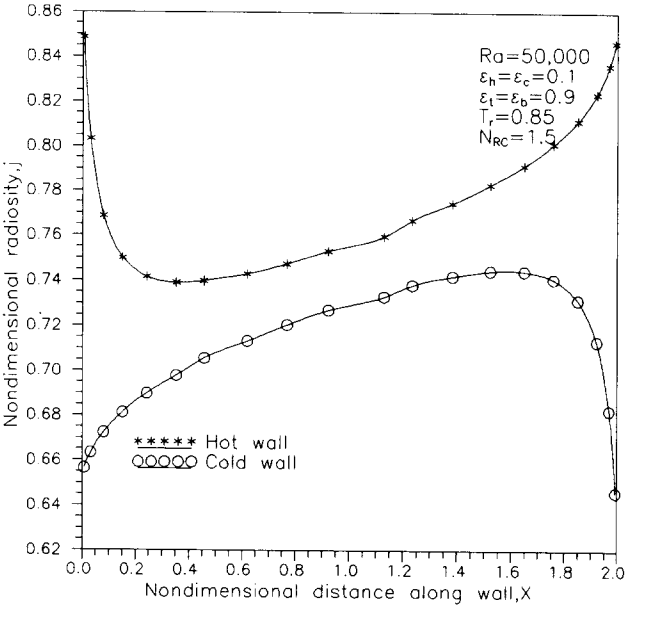

Figure 11 Nondimensional radiosity distribution along the side walls (low emissivity combination)

Table 3 Effect of radiation for Ra numbers of 50,000 and 75,000

Ra	$\overline{Nu}_f$ (Berkovsky & Polevikov)	$\overline{Nu}_f$ (with radiation present work)	$\overline{Nu}_f$ (Eckert & Carlson)
50,000	3.46	2.96	3.05
75,000	3.89	3.42	3.46

However, the emissivity of the side walls has been chosen as 0.1, corresponding to the value actually used in Eckert and Carlson's work. Table 3 compares the convective Nusselt number obtained by the use of the pure convection correlation of Berkovsky and Polevikov (1977), the experiment-based correlation of Eckert and Carlson (1961), and the convection Nusselt number obtained in the present study taking into account the presence of radiation. The agreement between the present values and Eckert's values, both of which are much smaller than the Berkovsky and Polevikov calculation, vindicates our earlier statement about the "dual" nature of radiation.

5.5. Effect of emissivity on the heat transfer characteristics of the cavity

For a parametric study of the effect of emissivity, we have chosen Ra = 50,000 and have computed results for five emissivities between 0.10 and 0.95 (Figure 12). It is evident that the convective drop decreases monotonically with emissivity, whereas the radiation Nusselt number increases monotonically and the two curves intersect each other at $\varepsilon_h = 0.229$. At this emissivity, radiation is as if absent, since its "dual" effects cancel each other. Also the simpler formulae such as the parallel-plate formula give radiation Nusselt numbers that are quite different from those obtained by rigorous calculations. The three-element enclosure model gives results that are not much different from the presently calculated result (in a three-element enclosure model, each side wall is assumed as one element and the top and bottom wall together are assumed as one element). However, we should mention that none of the above-mentioned simple formulae for the radiative heat transfer take into account the effect of convection, and hence they cannot predict the convective drop. Having established that radiation brings down the convection component, we can infer that all the simpler formulae overpredict the Nu_O.

5.6. The effect of radiation conduction interaction parameter on the heat transfer characteristics of the cavity

For a parametric study of the effect of N_{RC}, we have chosen the same set of fixed parameters, and N_{RC} has been varied from

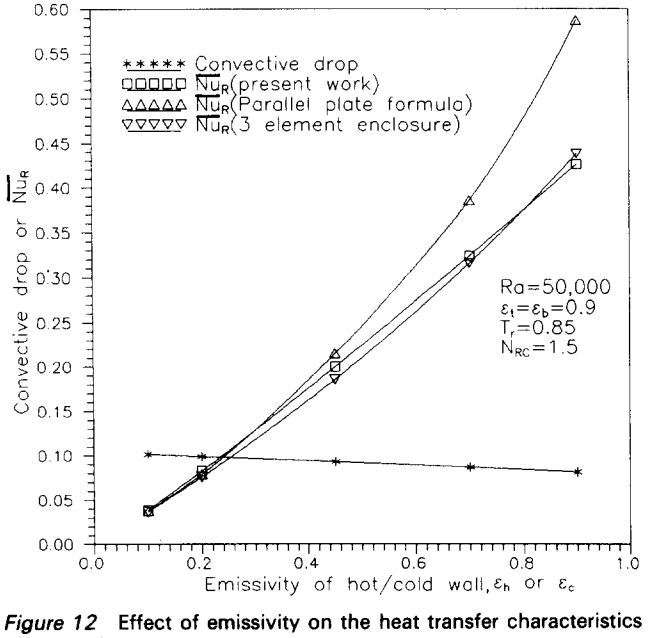

Figure 12 Effect of emissivity on the heat transfer characteristics of the cavity

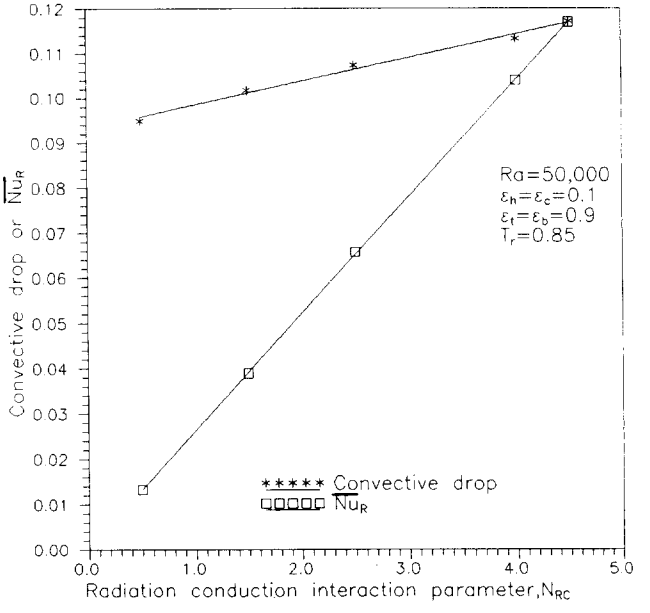

Figure 13 Effect of the radiation conduction interaction parameter on the heat transfer characteristics of the cavity

0.5 to 4.5. Figure 13 shows the variation of both the convective drop and the radiation Nusselt number with N_{RC}. It can be seen that at around $N_{RC} = 4.5$, the two effects cancel each other and radiation is as if absent. For the case of low N_{RC}'s, the convective drop is much higher compared to the radiation Nusselt number, hence, Nu_O is less with radiation than in the pure convection case for this set of fixed parameters, as shown in Figure 13.

5.7. The effect of temperature ratio on the heat transfer characteristics of the cavity

To probe into the effect of T_r on the heat transfer characteristics of the enclosure, the temperature ratio has been varied from 0.7 to 0.98 while keeping the other parameters fixed at values indicated in Figure 14. The case corresponds to the low

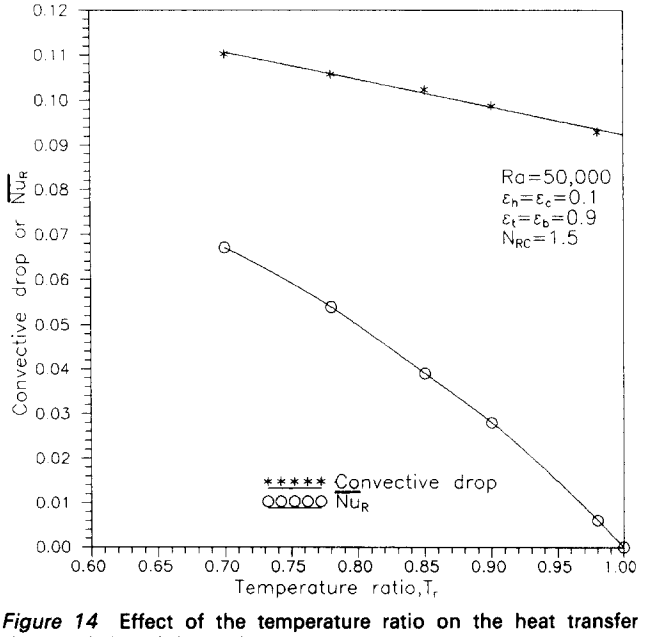

Figure 14 Effect of the temperature ratio on the heat transfer characteristics of the cavity

emissivity combination. Both the convective drop and the mean radiation Nusselt number come down with increasing T_r, but the convective drop for this particular combination of other parameters is much higher compared to the radiation Nusselt number. Hence the overall Nusselt number for this case is less than that for a pure convection case.

5.8. General comments

With these results in mind, a closer look into the existing correlations is indeed revealing. Let us take the case of Eckert and Carlson (1961). An MZ interferometer has been used to evaluate the heat transfer. It is known that interferometry gives only convective components. The fact that Eckert and Carlson's correlation runs 10 to 15 percent below other numerical correlations can be attributed to their measurement of only convective heat transfer, coupled with their neglect of surface radiation by numerical correlations. The cavity used in their work was 16 inches deep, with a maximum spacing of about 1.5 inches, with such a high width/spacing ratio, the three-dimensionality effect is expectedly negligible. The emissivities applicable to their setup correspond to the low emissivity combination in the present study, and hence the convective drop is significantly above the radiation Nusselt number.

Another very significant point emerges from the parametric analysis: the interaction between radiation and the free convection is so highly nonlinear that one does not know a priori whether the effect of radiation is to increase or decrease the overall heat transfer, and if so by what amount, unless the radiosity equations are solved and the coupling between convection and radiation is taken care of.

Concluding remarks

In this paper, the results of a numerical investigation have been presented for free convection in a square cavity, with special emphasis on the effect of surface radiation. The calculations that include radiation are more realistic, since it is impossible in practice to have surfaces with emissivities equal to zero. Radiation has a "dual" effect of contributing to the overall heat transfer as well as decreasing the convective component itself. Simple formulae that account for radiation in an additive way are not adequate, since they lead to large discrepancies even at small emissivities. Finally, an earnest attempt has been made to explain the possible source of discrepancies between the various available numerical correlations and the experimental results.

References

Asako, Y. and Nakamura, H. 1982. Heat transfer across a parallelogram shaped enclosure. *Bull. J.S.M.E.* **25**, 1412–1424

Bejan, A. 1984. Convective Heat Transfer. Wiley, New York

Berkovsky, B. M. and Polevikov, V. K. 1977. Numerical study of problems of high intensive free convection. In Turbulent Buoyant Flow and Convection, D. B. Spalding and N. Afghan (eds.), Volume 2. Hemisphere, Washington, 443–445

De Vahl Davis, G. and Jones, I. P. 1983. Natural convection in a square cavity. *Int. J. Numer. Methods Fluids*, **3**, 227–248

Eckert, E. R. G. and Carlson, W. O. 1961. Natural convection in an air layer. *Int. J. Heat Mass Transfer*, **2**, 106–120

Gebhart, B. et al. 1988. Buoyancy Induced Flows and Transport. Hemisphere, Washington

Gosman, A. D. et al. 1969. Heat and Mass Transfer in Recirculating Flows. Academic Press, London

Han, T. J. 1967. Numerical solutions for an isolated vortex in a slot and free convection across a square cavity. M.A.Sc Thesis, University of Toronto. Reported in Ostrach, S. 1972. Advances in Heat Transfer, J. P. Hartnett and H. Irving (eds.), Volume 8. Academic Press, London, 161–206

Hoogendoorn, C. J. 1985. Experimental methods in natural convection. In *Natural Convection, Fundamentals and Applications*, S. Kakac, W. Aung, and R. Viskanta (eds.). Hemisphere, Washington, 381–400

Hottel, H. C. and Sarofim, A. F. 1967. *Radiative Heat Transfer.* McGraw Hill, New York

Landis, F. and Rubel, A. 1970. Discussion on Newell & Schmidt [1970]. *ASME J. Heat Transfer*, **92**, 167–168

Lauriat, G. 1991. The effects of radiation on natural convection. *Int. Chem. Eng.*, **31**, 693–700

Newell, M. E. and Schmidt, F. W. 1970. Heat transfer in natural convection within rectangular enclosures. *ASME J. Heat Transfer*, **92**, 159–167

Shembarkar, T. R., Gururaja, J., and Krishna Prasad, K. 1977. Prandtl number effects on steady state natural convection flow and heat transfer in a square cavity. *Proc. 4th Natl. Heat and Mass Conf.*, Roorkee, India

Yang, K. T. and Lloyd, J. R. 1985. Natural convection radiation interaction in enclosures. In *Natural Convection, Fundamentals and Applications*, S. Kakac, W. Aung, and R. Viskanta (eds.). Hemisphere, Washington, 381–400